

DISCOVERY OF RADIO AFTERGLOW FROM THE MOST DISTANT COSMIC EXPLOSION

POONAM CHANDRA¹, DALE A. FRAIL², DEREK FOX³, SHRINIVAS KULKARNI⁴, EDO BERGER⁵, S. BRADLEY CENKO⁶,
DOUGLAS C.-J. BOCK⁷, FIONA HARRISON⁴, AND MANSI KASLIWAL⁴

¹ Department of Physics, Royal Military College of Canada, Kingston, ON, Canada; poonam.chandra@rmc.ca

² National Radio Astronomy Observatory, 1003 Lopezville Road, Socorro, NM 87801, USA

³ Department of Astronomy and Astrophysics, 525 Davey Laboratory, Pennsylvania State University, University Park, PA 16802, USA

⁴ Department of Astronomy, California Institute of Technology, Pasadena, CA 91125, USA

⁵ Harvard University, 60 Garden Street, Cambridge, MA 02138, USA

⁶ Department of Astronomy, 601 Campbell Hall, University of California, Berkeley, CA 94720-3411, USA

⁷ Combined Array for Research in Millimeter-wave Astronomy, P.O. Box 968, Big Pine, CA 93513, USA

Received 2009 September 2; accepted 2010 February 8; published 2010 February 26

ABSTRACT

We report on the discovery of radio afterglow emission from the gamma-ray burst GRB 090423, which exploded at a redshift of 8.3, making it the object with the highest known redshift in the universe. By combining our radio measurements with existing X-ray and infrared observations, we estimate the kinetic energy of the afterglow, the geometry of the outflow, and the density of the circumburst medium. Our best-fit model suggests a quasi-spherical, high-energy explosion in a low, constant-density medium. GRB 090423 had a similar energy release to the other well-studied high redshift GRB 050904 ($z = 6.26$), but their circumburst densities differ by 2 orders of magnitude. We compare the properties of GRB 090423 with a sample of gamma-ray bursts (GRBs) at moderate redshifts. We find that the high energy and afterglow properties of GRB 090423 are not sufficiently different from other GRBs to suggest a different kind of progenitor, such as a Population III (Pop III) star. However, we argue that it is not clear that the afterglow properties alone can provide convincing identification of Pop III progenitors. We suggest that the millimeter and centimeter radio detections of GRB 090423 at early times contained emission from the reverse shock. If true, this may have important implications for the detection of high-redshift GRBs by the next generation of radio facilities.

Key words: cosmology: observations – gamma-ray burst: general – hydrodynamics – radio continuum: general – stars: early-type

Online-only material: color figures

1. INTRODUCTION

Because of their extreme luminosities, gamma-ray bursts (GRBs) are detectable out to large distances, and due to their connection to core-collapse supernovae (SNe; Woosley & Bloom 2006), they could in principal reveal the stars that form from the first dark matter halos ($z \sim 20$ – 30) through the epoch of reionization at $z = 11 \pm 3$ and closer (Lamb & Reichart 2000; Ciardi & Loeb 2000; Gou et al. 2004; Inoue et al. 2007). As bright continuum sources, GRB afterglows also make ideal backlights to probe the intergalactic medium as well as the interstellar medium in their host galaxies. Predicted to occur at redshifts beyond those where quasars are expected, they could be used to study both the reionization history and the metal enrichment of the early universe (Totani et al. 2006).

The fraction of detectable GRBs that lie at high redshift ($z > 6$) is, however, expected to be small ($< 10\%$; Perley et al. 2009; Bromm & Loeb 2006). Until recently there were only two GRBs with measured redshifts $z > 6$: GRB 050904 (Kawai et al. 2006) and GRB 080913 (Greiner et al. 2009) with $z = 6.3$ and $z = 6.7$, respectively. However, on 2009 April 23 the *Swift* Burst Alert Telescope discovered GRB 090423, and the on-board X-ray Telescope (XRT) detected and localized a variable X-ray afterglow (Tanvir et al. 2009b; Salvaterra et al. 2009). In ground-based follow-up observations, no optical counterpart was found but a fading afterglow was detected by several groups at wavelengths longward of J band ($1.2 \mu\text{m}$). Based on both broadband photometry and near-infrared (NIR) spectroscopy,

the sharp optical/NIR drop-off was argued to be due to the $\text{Ly}\alpha$ absorption in the intergalactic medium, consistent with a redshift with a best-fit value of $z = 8.26^{+0.07}_{-0.08}$ (Tanvir et al. 2009b). The high redshift of GRB 090423 makes it the most distant observed GRB as well as the most distant object of any kind other than the cosmic microwave background. This event occurred approximately 630 million years after the big bang, confirming that massive stellar formation occurred in the very early universe.

In this Letter, we report on the discovery of the radio afterglow from GRB 090423 with the Very Large Array⁸ (VLA). Broadband afterglow observations provide constraints on the explosion energetics, geometry, and immediate environs of the progenitor star. The afterglow has a predictable temporal and spectral evolution that depends on the kinetic energy and geometry of the shock, the density structure of the circumburst environment, and shock microphysical parameters which depend on the physics of particle acceleration and the circumburst magnetic field. To the degree that we can predict differences in the explosion and circumburst media between GRB progenitors at high and low redshifts, we can search for these different signatures in their afterglows. This has been the motivation for previous multi-wavelength modeling of the highest- z afterglows (Frail et al. 2006; Gou et al. 2007).

⁸ The Very Large Array is operated by the National Radio Astronomy Observatory, a facility of the National Science Foundation operated under cooperative agreement by Associated Universities, Inc.

Table 1
Radio Observations of GRB 090423

Date (UT)	Δt (days)	Tel.	Freq. (GHz)	F_ν^a (μ Jy)	Int. Time ^b	Array Conf.
Apr 25.01	1.68	VLA	8.46	51 ± 45	13	B
Apr 26.08	2.75	VLA	8.46	-17 ± 37	16	B
May 01.05	7.72	VLA	8.46	74 ± 22	50	B
May 03.08	9.75	VLA	8.46	77 ± 18	75	B
May 03.98	10.65	VLA	8.46	57 ± 19	75	B
May 05.05	11.72	VLA	8.46	38 ± 19	71	B
May 05.99	12.66	VLA	8.46	87 ± 23	56	B
May 08.09	14.76	VLA	8.46	-4 ± 19	67	B
May 09.05	15.72	VLA	8.46	5 ± 18	71	B
May 10.08	16.75	VLA	8.46	73 ± 18	71	B
May 12.99	19.66	VLA	8.46	29 ± 18	70	B
May 14.10	20.77	VLA	8.46	88 ± 21	45	B
May 15.05	21.72	VLA	8.46	7 ± 15	110	B
May 20.13	26.80	VLA	8.46	42 ± 18	78	B
May 27.12	33.79	VLA	8.46	78 ± 19	77	BnC
Jun 01.11	38.78	VLA	8.46	44 ± 18	77	BnC
Jun 20.00	57.67	VLA	8.46	19 ± 21	78	C
Jun 26.08	63.75	VLA	8.46	49 ± 19	78	C
Jun 26.91	64.58	VLA	8.46	-4 ± 20	75	C
Apr 25.20	1.87	CARMA	92.5	450 ± 180

Notes.

^a Peak flux density at GRB 090423 position.

^b Integration time on GRB 090423 in minutes.

In order to investigate the nature of the GRB 090423 explosion, we combine our radio measurements with published X-ray and NIR observations and apply a model of the blast wave evolution to fit the afterglow data (Section 3). We compare the explosion energetics, circumburst density, and other derived characteristics to a sample of well-studied events and discuss prospects for using afterglow measurements to investigate the nature of high- z massive star progenitors.

2. OBSERVATIONS

2.1. Radio Observations

We began observing a field centered at the NIR afterglow of GRB 090423 with the VLA about one day after the burst (Chandra et al. 2009). Our first detection of the GRB afterglow was not until about one week later at a flux density of $73.8 \pm 21.7 \mu$ Jy. We continued to monitor the GRB with the VLA until it faded below detection on day 64.

In Table 1 we list the *individual* VLA measurements. In order to improve our detection sensitivity, we averaged several adjacent observations. Data sets were combined in the UV plane prior to imaging. By averaging three adjacent epochs (2009 May 1–May 3) when the afterglow was brightest, we estimate the best GRB position by fitting a two-dimensional Gaussian, which is R.A., decl. (J2000): $09^h55^m(33^s279 \pm 0^s005)$, $18^d08'(57'935 \pm 0'067)$. This position is consistent with an earlier, less accurate WFCAM-UKIRT position from Tanvir et al. (2009a).

Table 2 gives the flux densities at the averaged epochs. For all epochs, the flux density was measured at the position given above. We plot these data in Figure 1. There is a broad plateau of about 45μ Jy from 12 to 38 days, followed by a decline around day 55. The initial detections on days 8–10 could have contribution from a short-lived reverse shock (RS; Section 3).

We also observed GRB 090423 with the Combined Array for Research in Millimeter-wave Astronomy (CARMA) at the

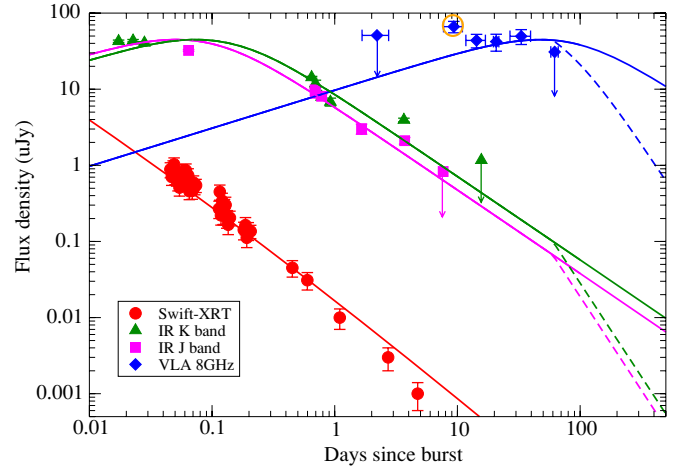


Figure 1. Multi-waveband observations for GRB 090423. The solid lines are best-fit light curves for the constant density isotropic model. The orange circled radio data likely have a contribution from RS (Section 3). Dashed lines show the model with a possible jet break around $t_j = 45$ d.

(A color version of this figure is available in the online journal.)

Table 2
VLA 8.5 GHz Flux Densities of GRB 090423 at Combined Epochs

Epochs Combined	Days Since Explosion	Flux Density (μ Jy)
Apr 25.01–Apr 26.08	2.21 ± 0.54	50.9 ± 30.9
May 01.05–May 03.98	9.34 ± 1.64	66.4 ± 11.4
May 05.05–May 10.08	14.32 ± 2.60	43.7 ± 8.9
May 12.99–May 15.05	20.71 ± 1.06	42.2 ± 10.6
May 20.13–Jun 01.11	33.12 ± 6.32	49.6 ± 11.0
Jun 20.00–Jun 26.91	62.00 ± 4.33	7.8 ± 11.6

95 GHz band on 2009 April 25.19 UT for 8 hr integration. Data were obtained under non-ideal weather conditions. The peak flux at the VLA afterglow position is $450 \pm 180 \mu$ Jy. Castro-Tirado et al. (2009) reported a secure millimeter band detection ($\lambda = 3$ mm) at a flux density of 200μ Jy with the Plateau de Bure Interferometer (PdBI) observed on 2009 April 23 and 24. Riechers et al. (2009) placed a flux upper limit of 0.96 mJy in the 250 MHz band observed with the Max-Planck-Millimeter Bolometer (MAMBO-2) array at the IRAM 30 m telescope. The Westerbork Synthesis Radio Telescope also observed the GRB between 2009 May 22.48 UT and 23.46 UT at 4.9 GHz and did not detect the afterglow (van der Horst 2009).

2.2. X-ray Observations

Swift-XRT (Burrows et al. 2005) observed the field of GRB 090423 for one week in photon counting mode. The XRT light curve is obtained from the online repository⁹ (Evans et al. 2007). The X-ray spectrum is well fit by a power-law model with a photon index $\Gamma = 2.05^{+0.14}_{-0.09}$ and a total column density of $N_H = (8.7 \pm 2.5) \times 10^{20} \text{ cm}^{-2}$ (Tanvir et al. 2009b; Krimm et al. 2009). We converted the 0.3–10.0 keV counts to a flux density at $E = 1.5$ keV ($\nu_0 = 3.6 \times 10^{17}$ Hz) using the above value for Γ and an unabsorbed count rate conversion of 1 count = $4.6 \times 10^{-11} \text{ erg cm}^{-2} \text{ s}^{-1}$.

2.3. Near-Infrared Observations

The NIR afterglow was observed by a variety of facilities worldwide; we have used values from Tanvir et al. (2009b). We

⁹ http://www.Swift.ac.uk/xrt_curves

have incorporated the Galactic extinction ($E(B - V) = 0.029$; Dickey & Lockman 1990) into these results.

3. RESULTS AND AFTERGLOW MODELING

Here, we combine our radio data with the existing X-ray and NIR data and model the afterglow evolution, interpreting it in terms of the relativistic blast wave model (Meszaros 2006). In this model, the afterglow physics is governed by the isotropic kinetic energy of the blast wave shock $E_{K,iso}$, the jet opening angle θ_j , the density of the circumburst medium n , and the microscopic parameters such as electron energy index p , and the fraction of the shock energy density in relativistic electrons ϵ_e and magnetic field ϵ_B . The afterglow modeling software (Yost et al. 2003) assumes a standard synchrotron forward shock formulation. In the X-ray band, we exclude the data before ~ 3900 s, since they contain a flare which is more likely due to the GRB itself than the afterglow.

It is well known (Sari et al. 1998, 1999; Chevalier & Li 1999) that the afterglow framework allows the above blast wave parameters to be constrained using multi-wavelength light curves. Here, we use a semianalytic approach to derive these constraints. First, we note the constancy of the peak flux density ($F_{\nu,max}$) between the NIR and the radio bands in Figure 1. If we interpret this as the passage of the synchrotron peak frequency ν_m through each band, this immediately rules out the wind model ($F_{\nu,max} \propto t^{-1/2}$) and favors a constant-density ambient medium ($F_{\nu,max} \propto t^0$). Another related constraint which comes from Figure 1 is the time of the peak in the NIR versus the radio bands. We note that in the NIR band, the light curve peaks at ~ 0.08 d. Thus if there was an early jet break, the model predicts that the synchrotron peak frequency ν_m would evolve from NIR to radio band around day 10 ($\nu_m \propto t^{-2}$); however, for the isotropic model ν_m should pass through the 8.5 GHz band around ~ 50 days ($\nu_m \propto t^{-3/2}$). Since radio light curve indeed peaks at about 50 days, this confirms that the jet break has not occurred at least until the afterglow peaked in radio band. The most important evidence of lack of early jet break comes from late time X-ray observations. A measurement of the X-ray flux with the *Chandra* satellite at approximately 36 days post-burst is consistent with a power-law extrapolation of the earlier *Swift*-XRT data (D. N. Burrows 2010, private communication) and implies $t_j > 36$ days (a late jet break, after the *Chandra* observation, is still allowed by the data).

Second, the declining part of the IR light curve is well fit by a power law with a decay index $\alpha = -1.10 \pm 0.27$. Whereas the overall X-ray light curve after 3900 s is well fit with a power-law index of $\alpha = -1.35 \pm 0.15$. For the isotropic, constant density model we expect the flux at a given frequency ν_{obs} to decline as $t^{3(1-p)/4}$ for $\nu_m < \nu_{obs} < \nu_c$ and $t^{(2-3p)/4}$ for $\nu_m < \nu_c < \nu_{obs}$, where ν_c is the synchrotron cooling frequency (Sari et al. 1998). These relations give consistent values of p for the NIR ($p = 2.46 \pm 0.36$) and X-ray ($p = 2.46 \pm 0.20$).

Finally, having obtained an estimation for p and determining the fact that the X-ray frequency has evolved past the cooling frequency $\nu_{X-ray} > \nu_c$, we can put a constraint on the total energy carried by the fireball electrons ($\epsilon_e E$) just from a single X-ray flux measurement. Using Equation (4) of Freedman & Waxman (2001) and X-ray flux on day 1, we obtain the fireball electron energy per unit solid angle in an opening angle $1/\Gamma$ on $t = 1$ d to be $\epsilon_e E/4\pi = 7.4 \times 10^{51}$ erg. If we assume $\epsilon_e = 1/3$ (Freedman & Waxman 2001), then the total fireball energy per unit solid angle in this opening will be $E/4\pi = 2.5 \times 10^{52}$ erg. However, we note that this is only an approximate estimation.

We summarize our robust inferences based on this preliminary analysis: (1) the data favor an isotropic explosion in a constant density medium, (2) the radio emission through most of the evolution is optically thin and provides only an upper limit on the synchrotron absorption frequency, (3) the cooling frequency lies between the IR and X-ray bands, (4) the afterglow kinetic energy is large. From Tanvir et al. (2009b) we also know that the extinction due to a putative host galaxy is negligible ($A_V < 0.08$).

We now move on to more detailed modeling (Yost et al. 2003) guided broadly by these preliminary results. We fit a constant density model for parameters: $E_{K,iso}$, θ_j , n , p , ϵ_e , and ϵ_B . All parameters were allowed to vary freely except that we fixed $p = 2.46$ to lie in a narrow range (± 0.20). The best-fit parameters using this semianalytic model are $E_K \approx 3.8 \times 10^{53}$ erg, $n \approx 0.9 \text{ cm}^{-3}$, $\epsilon_B(\%) \approx 1.6 \times 10^{-2}$, and $\epsilon_e \approx 0.28$. These values are only approximate and involve large uncertainties since we do not have good constraints on parameter ν_a .

This simple model provides a reasonable fit to the data and implies GRB kinetic energy to be $E_K = 3.8 \times 10^{53}$ erg. However, the last measured data point is around day 65 (radio band) and the last detections in the X-ray, radio, and NIR bands are at about day 36, day 40, and day 46 (Chary et al. 2009), respectively. Therefore a late jet break cannot be ruled out. To illustrate this more concretely, we overlay our best-fit model in Figure 1 with a late jet break $t_j \sim 45$ d. The implied jet opening angle $\theta_j > 0.21$ rad (Yost et al. 2003) reduces both the radiated and the kinetic energies of this event by a factor of ~ 45 . In this case, the isotropic equivalent gamma-ray energy $E_\gamma = 1 \times 10^{53}$ erg (von Kienlin 2009) and the blast wave kinetic energy $E_K = 3.8^{+9.8}_{-1.7} \times 10^{53}$ erg give *lower limits* to the beaming-corrected values of $E_\gamma > 2.2 \times 10^{51}$ erg and $E_K > 8.4^{+21.6}_{-3.7} \times 10^{51}$ erg, respectively.

The radio data point on day 9.34 ($t \sim 1$ day in the rest frame) has high flux and does not go through the best fit forward shock model. Such early, short-lived radio emission is fairly common in GRBs at lower redshifts and is thought to be due to a contribution from afterglow RS (Kulkarni et al. 1999; Soderberg & Ramirez-Ruiz 2003; Nakar & Piran 2004). We can make a rough estimate of the peak RS contribution for GRB 090423 using the formulation of Nakar & Piran (2004) and the best-fit parameters. The order of magnitude calculation shows that the RS contribution is expected to be $\sim 20 \mu\text{Jy}$. We note that this estimate may have large uncertainties. If we assume that the data on day 9.34 represent the peak of the RS, then this corresponds to a synchrotron self-absorption frequency of $\nu_a^r \sim 3.4 \times 10^{14}$ Hz. Using the scaling law for RS emission, $t_{radio} = \nu_a^r t_o / \nu_{radio}$, the time for RS peak in 90 GHz is $t \sim 0.87$ d. This implies that PdBI data flux reported by Castro-Tirado et al. (2009) may also have contribution from the RS.

4. DISCUSSION AND CONCLUSIONS

GRB 090423 is the highest-redshift object for which we have multi-wavelength observations, including good quality radio measurements. Below we address the following questions: based on its afterglow properties what can we learn about properties of the explosion and environs for this highest-redshift GRB? And, can we identify any differences between high and low redshift GRBs which indicate that they might arise from different progenitors? In particular, the initial generations of stars in the early universe are thought to be brighter, hotter, and more massive ($> 100 M_\odot$) than stars today (Haiman 2008;

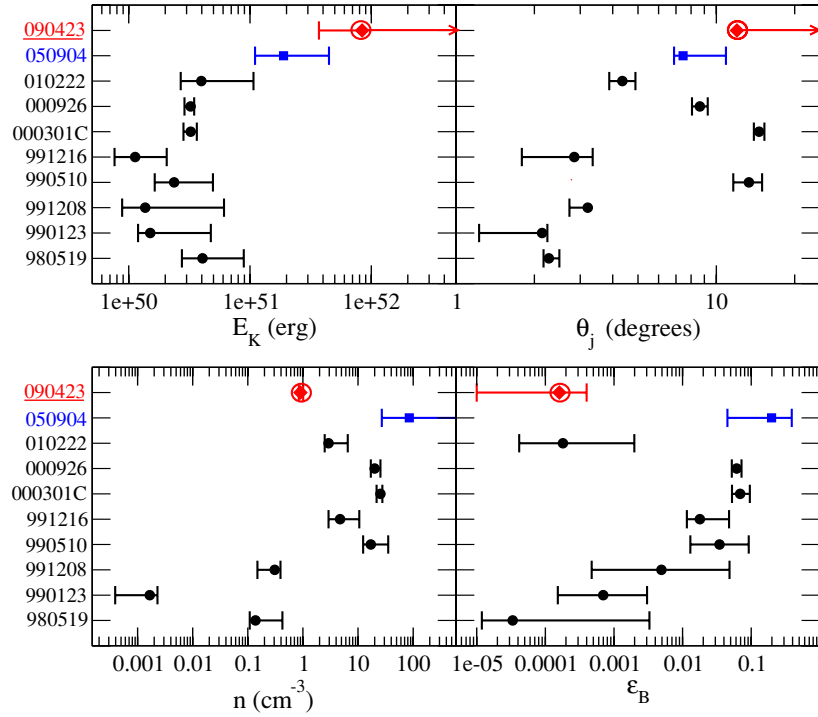


Figure 2. Comparison of GRB 090423 best-fit parameters with few moderate- z GRBs ($z \sim 1 - 3$) from Panaitescu & Kumar (2001) and with the high- z GRB 050904 ($z = 6.295$; Gou et al. 2007; Frail et al. 2006). Here, the upper limit on GRB 090423 E_K is $(3.8 + 9.8) \times 10^{51}$ erg. (A color version of this figure is available in the online journal.)

Bromm et al. 2009). Detecting these so-called Population III (Pop III) stars is one of the central observational challenges in modern cosmology, and the best prospect appears to be through observing their stellar death (Heger et al. 2003) via a supernova or GRB explosion. It is worth asking what observational signatures could signal a Pop III GRB.

Other than GRB 090423, only one other $z > 6$ event, GRB 050904 ($z = 6.26$), has high-quality broadband afterglow measurements. In Figure 2, we plot the best-fit parameters of these two GRBs along with a sample of well-studied lower redshift events from Panaitescu & Kumar (2001). Both high redshift bursts stand out in terms of their large blast wave energy ($> 10^{52}$ erg). We know from samples of well-studied afterglows (Frail et al. 2001; Panaitescu & Kumar 2001; Yost et al. 2003) that most have radiative and kinetic energies of order $\sim 10^{51}$ erg. In the collapsar model, the jet kinetic energy from a Pop III GRB could be 10–100 times larger than a Pop II event (Fryer et al. 2001; Heger et al. 2003). However, an energetic explosion does not appear to be an exclusive property of high- z GRBs. There is a growing population of bursts with energy $> 10^{52}$ erg, termed “hyper-energetic GRBs” (Cenko et al. 2010), which includes moderate- z events like GRB 070125 (Chandra et al. 2008) and GRB 050820A (Cenko et al. 2006).

Another potentially useful diagnostic is the density structure in the immediate environs of the progenitor star. The radio data are a sensitive in situ probe of the density because its emission samples the optically thick part of the synchrotron spectrum. The afterglows of GRB 090423 and GRB 050904 are best fit by a constant density medium and not one that is shaped by stellar mass loss (Chevalier & Li 1999). The density obtained for GRB 050904 was the highest seen ($n \approx 84 - 680 \text{ cm}^{-3}$) for any GRB to date, while GRB 090423 with $n = 0.9 \text{ cm}^{-3}$ does not stand out (Figure 2), indicating these two high redshift bursts exploded in very different environments. A circumburst density

of the order one particle per cc is predicted for Pop III stars, since this density is limited by strong radiation pressure in the mini halo from which the star was formed (Bromm et al. 2003). This is not a unique property, since many local SNe explode in tenuous media, and so density constraints are not useful to signal Pop III explosions.

For the other afterglow parameters (p , ϵ_e , ϵ_B , and θ_j) there are no published predictions for how they may differ between different progenitor models. Thus, we turn to considering the prompt high-energy emission of GRB 090423.

Salvaterra et al. (2009) and Tanvir et al. (2009b) both noted that the high-energy properties of GRB 090423 (fluence, luminosity, duration, radiative energy) are not substantially different from those moderate- z GRBs. We are not aware of any quantitative predictions based on these observed properties that would discriminate between Pop II and Pop III progenitors. For example, apart from the effect of $(1 + z)$ time dilation, there is no reason to expect high- z GRBs to have significantly longer intrinsic durations. Collapsar models which form black holes promptly through accretion onto the proto-neutron star (Type I) or via direct massive ($> 260 M_\odot$) black hole formation (Type III) have durations set by jet propagation and disk viscosity timescales, respectively (MacFadyen et al. 2001; Fryer et al. 2001), which are ~ 10 s in the rest frame (with large uncertainties; Fryer et al. 2001).

Metallicity can also be an important discriminant. There is a critical metallicity ($Z > 10^{-3.5} Z_\odot$) below which high-mass Pop III stars dominate (Bromm et al. 2009; Bromm & Loeb 2006). The contribution of Pop III stars to the comoving star formation rate is expected to peak around $z = 15$ but their redshift distribution exhibits a considerable spread to $z \sim 7$. Thus, we might find high-redshift GRBs with Pop III progenitors in “pockets” of low metallicity. Salvaterra et al. (2009) argue for a lower bound of $Z > 0.04 Z_\odot$ based on their detection

of excess soft X-ray absorption by metals along the line of sight, in comparison to the Milky Way column density predicted from H I (21 cm) measurements. We do not consider this a robust measurement as it is sensitive to a range of unaccounted-for systematic effects, including spectral variability, spectral curvature, low-amplitude X-ray flares, and the presence of intervening (cosmological) absorption systems along the line of sight.

Summarizing the above discussion, we do not find that the individual properties of GRB 090423 are sufficiently dissimilar to other GRBs to warrant identifying it as anything other than a normal GRB. We lack robust predictions of well-defined afterglow signatures that could allow us to unambiguously identify a Pop III progenitor star from its afterglow properties alone. Significantly larger numbers of GRBs at high redshift with well-sampled afterglow light curves, high-resolution spectra, and host galaxy detections are needed to determine if high-redshift GRB progenitors differ in a statistical sense from those at low redshift.

We note that like GRB 050904, the GRB 090423 afterglow indicates the possible signature of RS emission in the radio, in VLA, and PdBI data. Inoue et al. (2007) have studied the expected RS emission at high redshift, and they find that the effects of time dilation almost compensate for frequency redshift, resulting in a near-constant observed peak frequency in the mm band ($\nu \sim 200$ GHz) at a few hours post-event, and a flux at this frequency that is almost independent of redshift. Further, the mm band does not suffer significantly either from extinction (in contrast to the optical) or scintillation (in contrast to the radio). Therefore, detection of mm flux at a few hours post-event should be a good method of indicating a high-redshift explosion. ALMA, with its high sensitivity ($\sim 75 \mu\text{Jy}$ in 4 minutes), will be a potential tool for selecting potential high- z bursts that would be high priority for intense follow-up across the spectrum. This will hopefully greatly increase the rate at which high- z events are identified.

Finally, our data do not rule out a late jet break at $t_j > 45$ days, which, as discussed above, makes the total explosion energy uncertain. Extremely sensitive VLA observations would be required to distinguish between the isotropic versus jet model. However, in 2010 with an order of magnitude enhanced sensitivity the EVLA will be the perfect instrument for such studies. For a 2 hr integration in the 8 GHz band, the EVLA can reach sensitivity up to $2.3 \mu\text{Jy}$ which will be able to detect the GRB 090423 for 2 years or 6 months if the burst is isotropic or jet-like, respectively. EVLA will thus be able to detect fainter events and follow events like GRB 050904 and GRB 090423 for a longer duration, therefore obtaining better density measurements, better estimates of outflow geometry, and the total kinetic energy.

We thank the referee for useful comments. We thank Bob Dickman for allocation of VLA time and Joan Wrobel and Mark Claussen for scheduling the observations. This work made use of data supplied by the UK Swift Science Data Centre at the University of Leicester. P.C. is supported by NSERC Discovery grants and DND-ARP grants held by Kristine Spekkens and Gregg Wade at RMC of Canada.

REFERENCES

- Bromm, V., & Loeb, A. 2006, *ApJ*, **642**, 382
 Bromm, V., Yoshida, N., & Hernquist, L. 2003, *ApJ*, **596**, L135
 Bromm, V., Yoshida, N., Hernquist, L., & McKee, C. F. 2009, *Nature*, **459**, 49
 Burrows, D. N., et al. 2005, *Space Sci. Rev.*, **120**, 165
 Castro-Tirado, A. J., et al. 2009, *GCN Circ.*, **9273**, 1
 Cenko, S. B., et al. 2006, *ApJ*, **652**, 490
 Cenko, S. B., et al. 2010, *ApJ*, **711**, 641
 Chandra, P., Frail, D. A., & Kulkarni, S. R. 2009, *GCN Circ.*, **9249**, 1
 Chandra, P., et al. 2008, *ApJ*, **683**, 924
 Chary, R., et al. 2009, *GCN Circ.*, **9582**, 1
 Chevalier, R. A., & Li, Z.-Y. 1999, *ApJ*, **520**, L29
 Ciardi, B., & Loeb, A. 2000, *ApJ*, **540**, 687
 Dickey, J. M., & Lockman, F. J. 1990, *ARA&A*, **28**, 215
 Evans, P. A., et al. 2007, *A&A*, **469**, 379
 Frail, D. A., et al. 2001, *ApJ*, **562**, L55
 Frail, D. A., et al. 2006, *ApJ*, **646**, L99
 Freedman, D. L., & Waxman, E. 2001, *ApJ*, **547**, 922
 Fryer, C. L., Woosley, S. E., & Heger, A. 2001, *ApJ*, **550**, 372
 Gou, L.-J., Fox, D. B., & Mészáros, P. 2007, *ApJ*, **668**, 1083
 Gou, L. J., Mészáros, P., Abel, T., & Zhang, B. 2004, *ApJ*, **604**, 508
 Greiner, J., et al. 2009, *ApJ*, **693**, 1610
 Haiman, Z. 2008, in *Astrophysics & Space Science Library*, ed. H. Thronson, A. Tielens, & M. Stiavelli (Dordrecht: Springer)
 Heger, A., et al. 2003, *ApJ*, **591**, 288
 Inoue, S., Omukai, K., & Ciardi, B. 2007, *MNRAS*, **380**, 1715
 Kawai, N., et al. 2006, *Nature*, **440**, 184
 Krimm, H. A., et al. 2009, *GCN Rep.*, **211**, 2
 Kulkarni, S. R., et al. 1999, *ApJ*, **522**, L97
 Lamb, D. Q., & Reichart, D. E. 2000, *ApJ*, **536**, 1
 MacFadyen, A. I., Woosley, S. E., & Heger, A. 2001, *ApJ*, **550**, 410
 Meszaros, P. 2006, *Rep. Prog. Phys.*, **69**, 2259
 Nakar, E., & Piran, T. 2004, *MNRAS*, **353**, 647
 Panaitescu, A., & Kumar, P. 2001, *ApJ*, **554**, 667
 Perley, D. A., et al. 2009, *AJ*, **138**, 1690
 Riechers, D. A., et al. 2009, *GCN Circ.*, **9322**, 1
 Salvaterra, R., et al. 2009, *Nature*, **461**, 1258
 Sari, R., Piran, T., & Halpern, J. P. 1999, *ApJ*, **519**, L17
 Sari, R., Piran, T., & Narayan, R. 1998, *ApJ*, **497**, L17
 Soderberg, A. M., & Ramirez-Ruiz, E. 2003, *MNRAS*, **345**, 854
 Tanvir, N., Levan, A., Kerr, T., & Wold, T. 2009a, *GCN Circ.*, **9202**, 1
 Tanvir, N. R., et al. 2009b, *Nature*, **461**, 1254
 Totani, T., et al. 2006, *PASJ*, **58**, 485
 van der Horst, A. J. 2009, *GCN Circ.*, **9503**, 1
 von Kienlin, A. 2009, *GCN Circ.*, **9251**, 1
 Woosley, S. E., & Bloom, J. S. 2006, *ARA&A*, **44**, 507
 Yost, S. A., Harrison, F. A., Sari, R., & Frail, D. A. 2003, *ApJ*, **597**, 459